Kelvin Wave Time Scale Propagation Features of the Madden-Julian Oscillation as Measured by the Chen-MJO Index

James A. Ridout and Maria K. Flatau
Naval Research Laboratory, Monterey, CA

Corresponding author's e-mail:
James.Ridout@nrlmry.navy.mil

Summary:

For further information, please see:
Ridout, J. A., and M. K. Flatau (2011), Convectively coupled Kelvin wave propagation past Sumatra: A June case and corresponding composite analysis, J. Geophys. Res., 116, D07106, doi:10.1029/2010JD014981
Ridout, J. A., and M. K. Flatau (2011), Kelvin wave time scale propagation features of the Madden-Julian Oscillation (MJO) as measured by the Chen-MJO index, J. Geophys. Res., 116, D18102, doi:10.1029/2011JD015925

Kelvin wave time scale propagation features in an indexed measure of the strength of the Madden-Julian Oscillation (MJO) are investigated. Examination of reanalysis data and Chen-MJO index data for three 14 May to 21 Sep. periods shows that recurring divergence events near Sumatra (denoted here as "**Sumatra Divergence Events" (SDEs)**) frequently associated with **convectively coupled Kelvin waves (CCKWs)** tend to correspond in a time-lagged manner with increases in indexed MJO strength at various longitudes. A similar signal is demonstrated in a 32-year data set of the Chen-MJO index by examining time-lagged correlations between increases in indexed MJO strength at various longitudes and corresponding increases for selected "**MJO Index Events**" **(MIEs)** at 80°E and 160°E. Although possible alternative explanations exist, the results are consistent with an enhanced rate of increase in MJO strength as the apparent Kelvin wave signal passes, roughly marking the beginning of an extended period of MJO growth. A look at a particular MJO episode provides evidence consistent with this view of the statistical results, while supporting a role of sequential CC Kelvin wave passages in the propagation of the MJO.

"Sumatra Divergence Event" (SDE) Case Study

An episode of large-scale low-level divergence on 18 June, 2006 was studied using a 12-km grid reanalysis data set from the Coupled Ocean Atmosphere Mesoscale Prediction System (COAMPS®[1]) . Radar data from CloudSat (*Stephens et al*., 2002) and rainfall data from the Tropical Rainfall Measuring Mission (TRMM) (e.g., *Simpson et al*., 1988) (not shown here) point to impacts of a transition to stratiform convection, possibly influenced in part by interaction with an equatorial Rossby wave (*Ridout and Flatau* (2011a).

[1]COAMPS® is a registered trademark of the Naval Research Laboratory.

Event of 18 June, 2006 - Divergence and Stratiform Convection

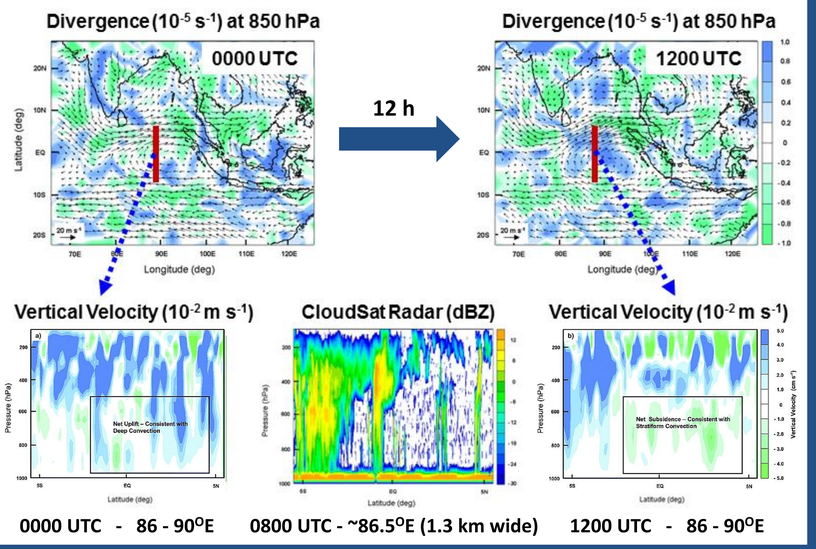

SDE Composite

A number of events sharing similar dynamical features with the SDE of 18 June, 2006 were identified by searching reanalysis data. An SDE composite was thus constructed using data from three 14 May to 21 Sep. periods (2006, 2008, 2009). For 2006, the data used were the COAMPS 12-km grid reanalysis data averaged to a 2.5° x 2.5° grid. For 2008 and 2009, data from the ECMWF reanalysis dataset provided for the Year of Tropical Convection (YOTC) Program (*Waliser and Moncrieff*, 2008), similarly averaged, were used.

Selection of SDE "Composite Events"

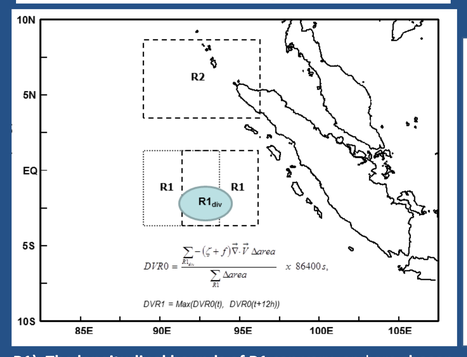

R1) The longitudinal bounds of R1 can vary, and are **chosen to maximize vorticity change due to divergence within $R1_{div}$**, the portion of R1 where at each point **positive divergence at time *t* contributes to an observed net decrease in negative vorticity in $R1_{div}$** during the 24 h period centered at time *t*. Within R1, the contribution to vorticity change at time *t* by divergence is required to be dominated by the (positive) contribution (DVR1) from $R1_{div}$.

R2) The net change in vorticity in R2 is required to be negative for the 24 h period centered at time *t*, as well as for the following 24 h. The area of positive absolute vorticity in R2 at time *t* must exceed the area of negative absolute vorticity (**roughly equivalent to the local dynamic equator lying to the south of the northern tip of Sumatra**).

Association of SDE events (DVR1 values) with Kelvin wave rainfall

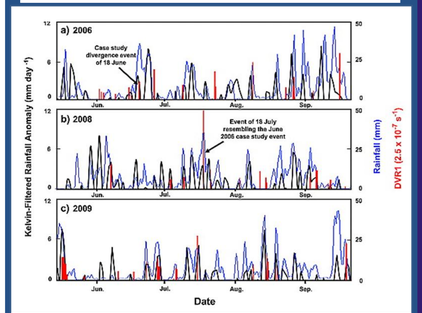

Composite event values of DVR1 (2.5×10^{-7} s^{-1}) (red), rainfall (blue) (mm) within the area from which R1 is selected, and positive values of the Kelvin wave filtered rainfall anomaly (black) computed at 98°E for rainfall between 5°N - 5°S, for 14 May - 21 Sep. periods of (a) 2006, (b) 2008, and (c) 2009.

Kelvin-wave signal in Chen-MJO Index

The SDE case study and composite analysis suggest that for the boreal summertime, large values of DVR1 may often reflect expansion at low levels of a cyclonic circulation near Sumatra as it uncouples from passing CCKWs. Large values of DVR1 might thus tend to correspond to "flow conditioning" for subsequent CCKWs (as suggested for the 18 June, 2006 SDE). Considering potential impacts of coupling of CCKWs with the MJO [e.g., *Majda and Biello*, 2004], enhanced MJO propagation eastward could result. Evidence in this regard can be seen in time-lagged correlations between DVR1 and increases in **"MJO strength" (as measured by the negative of the Chen-MJO index** (*Chen and Del Genio*, 2008)).

Kelvin wave signal in time-lagged correlations between DVR1 and increases in MJO Strength

The approximate 18 m s^{-1} phase velocity suggested by the correlation peaks is consistent with (convectively coupled) Kelvin wave time scale eastward propagation (*Wheeler and Kiladis*, 1999)

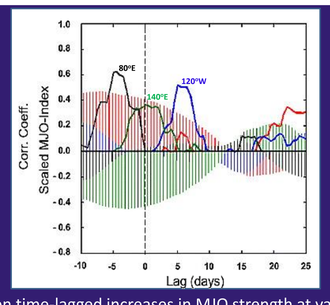

Pearson correlation coefficients (positive values) between time-lagged increases in MJO strength at various longitudes and values of DVR1 from SDEs. Black curve, results for 80°E; green curve, 140°E; blue curve, 120°W; red curve, 10°W. The corresponding values of the scaled Chen-MJO index are also plotted (bars).

Evidence of a CCKW signal can be further observed directly from the 32-year dataset of the Chen-MJO index available from the Climate Prediction Center (CPC). To see this, **MJO Index Events (MIEs)** were selected using a simple tuning procedure based on maximizing correlations between MJO strength increases at a given reference longitude and 120°W.

Kelvin wave signal in time-lagged correlations between increases in MJO Strength and MJO strength increases for MIEs

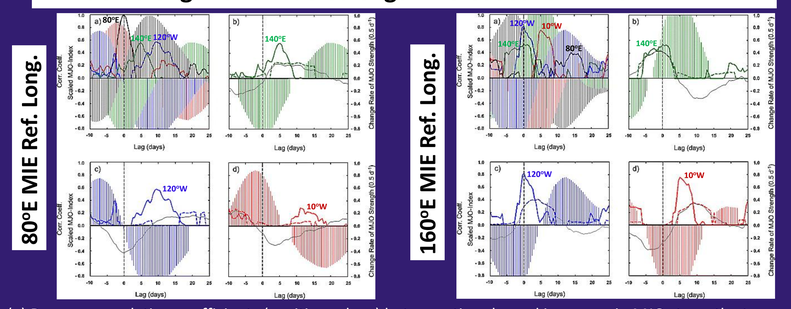

(a) Pearson correlation coefficients (positive values) between time-lagged increases in MJO strength at various (color-coded as above) longitudes and increases in MJO strength for the MIEs. Corresponding values of the scaled MJO index are also plotted (bars). The data from (a) are reproduced in (b) 140°E, (c) 120°W, and (d) 10°W along with additional data: positive contributions to changes in MJO strength (dashed curves) and the total mean change rate in MJO strength (thin solid black curves). In (b–d), the Chen-MJO index data and contributions to positive changes in MJO strength are filtered so that nonzero values represent statistically significant (95% level) deviations from the corresponding means over all lag times.

CCKW context

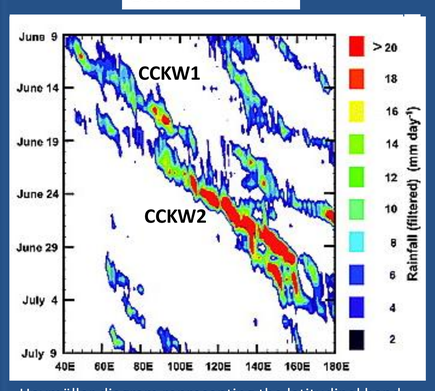

Hovmöller diagram representing the latitudinal band 0–10°N for 9 June to 9 July 2006, showing the positive eastward propagating component of Fourier-filtered TRMM rainfall rates (mm d^{-1}).

Impact on vorticity

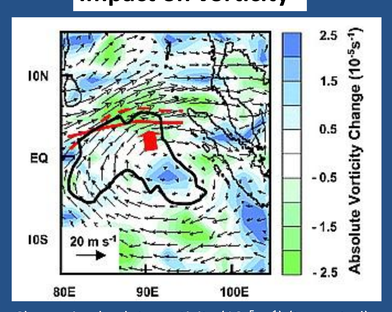

Change in absolute vorticity (10^{-5} s^{-1}) (truncated) at 850 hPa during the 24 h period beginning at 0000 UTC on 18 June 2006. The 850 hPa wind field vectors at the end of the period are also plotted. The area of positive divergence at 850 hPa within the vortex at 1200 UTC is roughly outlined (thick black curve). The northward movement of the dynamic equator at 850 hPa during the 24 h period centered at 1200 UTC is depicted in red.

Composite Temporal Development

Rainfall and 850 hPa Divergence Consistent with CCKW Passage

850 hPa Absolute Vorticity and Winds Dynamic Equator Extends Northward ~3 deg.

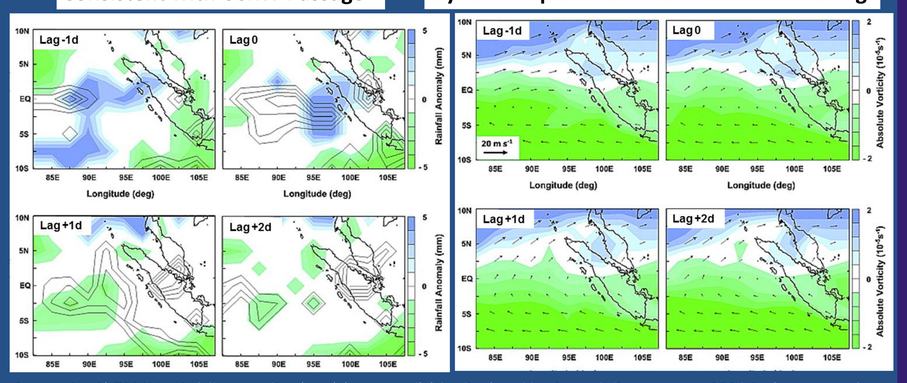

Composite A) TRMM rainfall anomalies (mm) (truncated) (shading) and horizontal divergence at 850 hPa (contours of positive values only; contour interval is 0.6×10^{-6} s^{-1}) and B) absolute vorticity (10^{-5} s^{-1}) (truncated) (shading) and horizontal wind field vectors at 850 hPa for four lag times with respect to the composite events: (a) −1 day, (b) 0 days, (c) +1 day, and (d) +2 days. Spatial and temporal variations in the plots represent contributions of statistically significant (95% level) deviations from area and time means.

Shift in the dynamic equator following passage of CCKW1

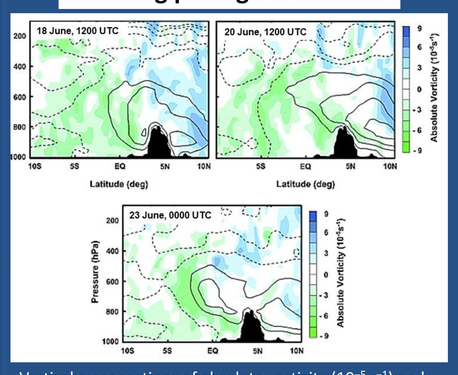

Vertical cross sections of absolute vorticity (10^{-5} s^{-1}) and zonal wind (m s^{-1}) (cont. interval is 5 m s^{-1}, zero cont. omitted, dashed curves denote negative values). Plots represent data averaged between 92.5°E - 97.5°E.

Propagation of CCKW2 may reflect impact of flow conditioning by the shift in the dynamic equator

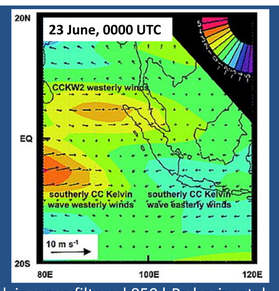

Kelvin wave filtered 850 hPa horizontal wind field vectors computed from the NCEP/NCAR reanalysis . The zonal component is indicated by shading (m s^{-1}).

SDE strength (DVR1) better correlated with *increases* in MJO strength than with MJO strength

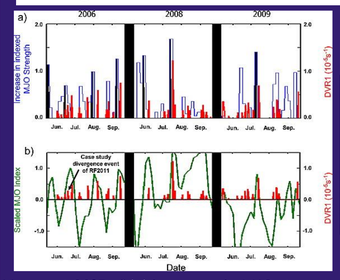

Values at 80°E of (a) increases in MJO strength for all cases (blue), and for the MIEs (black), and (b) scaled MJO index (green). Values of DVR1 (10^{-7} s^{-1}) in red.

CCKW1 rainfall observed along the leading edge of MJO convection, consistent with statistical results for MIEs. CCKW2 passage supports a role of multiple CCKWs in the MJO, as suggested by previous studies.

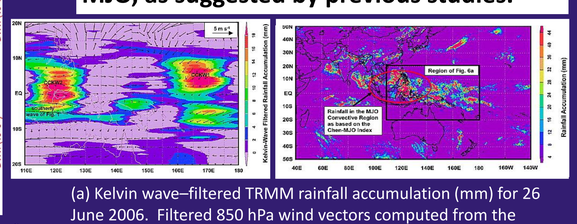

(a) Kelvin wave–filtered TRMM rainfall accumulation (mm) for 26 June 2006. Filtered 850 hPa wind vectors computed from the NCEP/NCAR reanalysis at 00:00 UTC on 26 June are also shown. The approximate locations of Kelvin wave rainfall associated with waves CCKW1 and CCKW2 are indicated. (b) Total rainfall (mm) on 26 June.

References

Chen, Y., and A. D. Del Genio (2008), Evaluation of tropical cloud regimes in observations and a general circulation model, Clim. Dyn., 32, 355–369, doi:10.1007/s00382-008-0386-6.

Majda, A. J., and J. A. Biello (2004), A multi-scale model for tropical intraseasonal oscillations, Proc. Natl. Acad. Sci. U. S. A., 101, 4736–4741, doi:10.1073/pnas.0401034101.

Ridout, J. A., and M. K. Flatau (2011a), Convectively coupled Kelvin wave propagation past Sumatra: A June case and corresponding composite analysis, J. Geophys. Res., 116, D07106, doi:10.1029/ 2010JD014981.

Ridout, J. A., and M. K. Flatau (2011b), Kelvin wave time scale propagation features of the Madden-Julian Oscillation (MJO) as measured by the Chen-MJO index, J. Geophys. Res., 116, D18102, doi:10.1029/ 2011JD015925.

Simpson, J., R. F. Adler, and G. R. North (1988), Proposed Tropical Rainfall Measuring Mission (TRMM) satellite, Bull. Am. Meteorol. Soc., 69, 278–295, doi:10.1175/1520-0477(1988)069<0278:APTRMM> 2.0.CO;2.

Stephens, G. L., et al. (2002), The CloudSat Mission and the A-Train, Bull. Am. Meteorol. Soc., 83, 1771–1790, doi:10.1175/BAMS-83-12-1771.

Waliser, D. E., and M. Moncrieff (2008), The Year of Tropical Convection (YOTC) science plan: A joint WCRP-WWRP/THORPEX international initiative, Rep. WMO/TD 1452, World Meteorol. Organ., Geneva, Switzerland.

Wheeler, M., and G. N. Kiladis (1999), Convectively coupled equatorial waves: Analysis of clouds and temperature in the wavenumber-frequency domain, J. Atmos. Sci., 56, 374–399, doi:10.1175/1520-0469(1999)056<0374:CCEWAO>2.0.CO;2.

The ECMWF data were provided by ECMWF for the YOTC program and were obtained from their Web site at http://data-portal.ecmwf.int/data/d/yotc_od/. The NCEP reanalysis data were provided by the NOAA OAR ESRL PSD, Boulder, Colorado, and were obtained from their Web site at http://www.esrl.noaa.gov/psd/. The MJO index data (Chen-MJO index) were obtained from the Web site of the National Weather Service Climate Prediction Center (CPC) (http://www.cpc.noaa.gov/products/precip/CWlink/daily_mjo_index/pentad.html). The TRMM rainfall data were acquired using the GES DISC Interactive Online Visualization and Analysis Infrastructure (Giovanni), a part of the NASA Goddard Earth Sciences (GES) Data and Information Services Center (DISC). This research was sponsored by the Naval Research Laboratory under program element 0601153N. The work was supported in part by a grant of computing time from the Department of Defense's High Performance Computing Program.